

INVESTIGATION OF COUPLED EFFECTS OF TEMPERATURE AND RELATIVE HUMIDITY ON DYNAMIC PERFORMANCE OF MEMS BEAM RESONATORS IN GAS RAREFACTION

Nguyen Chi Cuong*, Trinh Xuan Thang, Truong Van Phat, Vu Manh Giap,
Ngo Vo Ke Thanh

Research Laboratories of Saigon High-Tech-Park, Lot I3, N2 Street, Saigon Hi-Tech-Park,
District 9, Ho Chi Minh city

*Email: cuong.nguyenchi@shtplabs.org

Received: 23 September 2018; Accepted for publication: 11 April 2019

Abstract. The modified molecular gas lubrication (MMGL) equation with the effective viscosity of moist air is utilized to solve for the squeeze film damping (SFD) problem on the dynamic performance of MEMS resonators. Thus, the coupled effects of temperature and relative humidity are discussed on the Q -factors of MEMS resonators in a wide range of gas rarefaction (pressure, p and accommodation coefficients (ACs)) and resonant mode of vibration. The results showed that the Q -factor of moist air decreases more significantly as temperature and relative humidity increase at higher gas rarefaction (lower p , and ACs) conditions.

Keywords: MEMS resonators, Quality factor, relative humidity, temperature, gas rarefaction.

Classification numbers: 5.2.4, 5.4.3, 5.4.4.

1. INTRODUCTION

Micro-electro-mechanical systems (MEMS) beam (such as MEMS bridge, cantilever, etc.), which is the most popular structure of resonators, are successfully used in numerous miniaturized sensor and detector applications [1, 2].

In MEMS resonators, the most important dynamic characteristic of resonator is the quality factor (Q -factor). Higher Q -factor (lower energy loss), which is important requirement of MEMS resonators for higher sensitivity and long-term stability of sensing systems. There are several kinds of damping mechanism of oscillating structures that minimized the Q -factor of MEMS resonators. In air ambient environment, the external squeeze film damping (SFD), which is a dominant damping source appeared as the gas flow squeezed in small gas film spacing between two structural surfaces due to the normal motion process [3]. The internal structure damping sources such as the thermoelastic damping (TED) (loss into the structure) [4] and support loss (loss into the substrate) [5] are the other dominant damping mechanisms. The SFD is strongly influenced by the ambient pressure and gas rarefaction which are functions of the environmental effects (such as temperature and humidity).

In air atmospheric pressure, the temperature and humidity of moist air are the main problems on beam dynamics which are strongly influenced by the viscous damping. Many studies have investigated the effect of temperature on the dynamic performances of MEMS resonators [6-8]. Few studies have considered the coupled effects of temperature and humidity on the Q -factor of MEMS resonators in gas atmospheric air [9,10]. Recently, Hasan et al. [11] has studied the effects of temperature and relative humidity on the dynamic response of MEMS resonator at atmospheric pressure condition. The obtained results showed that the Q -factor of MEMS resonators changed with temperature and humidity of moist air. Moreover, the influences of temperature and relative humidity on the Q -factor of MEMS resonators in gas rarefaction are not discussed yet.

In gas rarefied flow, low pressure (p) is introduced into very small gap film spacing (h) to reduce the SFD. The mean free path (λ) of gas flow enhances considerably, then the slip flow takes place on the solid surfaces. To consider the gas rarefaction effect, the so-called effective viscosity ($\mu_{eff} = \mu/Q_p$) is introduced to replace the primary dynamic viscosity (μ) and Poiseuille flow rate for gas rarefaction corrector (Q_p). Fundamentally, the effect of gas rarefaction characterized by the Knudsen number ($K_n = \lambda/h$), which presents for various gas rarefied regions and surface accommodation coefficients, ACs (α), which present for the average tangential momentum exchanges of the gas molecular and solid surfaces interaction. Detail review of the gas rarefaction effects is introduced in [12-14]. Recently, Haider et al. [15] found that the effective viscosity (μ_{eff}) changed considerably with temperature and relative humidity of moist air. Therefore, the influences of temperature and relative humidity in gas rarefaction must be carefully considered to improve the Q -factor of MEMS resonators.

In the previous work, the quality factors of MEMS resonators are obtained by solving the modified molecular gas lubrication (MMGL) equation and the transverse vibration equation of micro-structure simultaneously in the eigenvalue problem [12]. The effects of gas rarefaction [12] and surface roughness [13] are discussed on the Q -factors of MEMS resonators. Also, the influence of temperature [14] and relative humidity of moist air [16] are considered as important effects on the Q -factors of MEMS resonators in gas rarefaction by modifying the MMGL equation using the dynamic viscosity (μ) and Poiseuille flow rate (Q_p) as functions of temperature (T) and relative humidity (RH), respectively. In this study, the MMGL equation is modified with the effective viscosity ($\mu_{eff}(RH, T) = \mu(RH, T)/Q_p(RH, T)$) with the dynamic viscosity ($\mu(RH, T)$) in [17] and databases for Poiseuille flow rate ($Q_p(RH, T)$) [18] changed as functions of both temperature (T) and relative humidity (RH). Thus, the present model, is a new model to consider the coupled effects of temperature and relative humidity by using the effective viscosity ($\mu_{eff}(RH, T)$) in higher gas rarefaction conditions, can be applicable in modeling and simulation of MEMS and NEMS devices. The internal structural damping (TED and support loss) are also included. Finally, the influences of temperature and relative humidity are discussed on the Q -factors and weighting of SFD of MEMS resonators in wide range of gas rarefaction (pressure (p), and ACs (α_1, α_2)). The obtained results can be utilized to design the high Q -factor of MEMS temperature and humidity sensors based on the beam structure operating in a wide range of resonant mode of vibration and gas rarefaction conditions.

2. MATERIALS AND METHODS

2.1. The MMGL equation for the SFD problem

In gas atmospheric environment, the harmonic vibration of micro-beam is restricted as the gas flow trapped in small gap film spacing between the vibrational micro-beam and the stationary substrate during their transverse vibration process as showed in Figure 1.

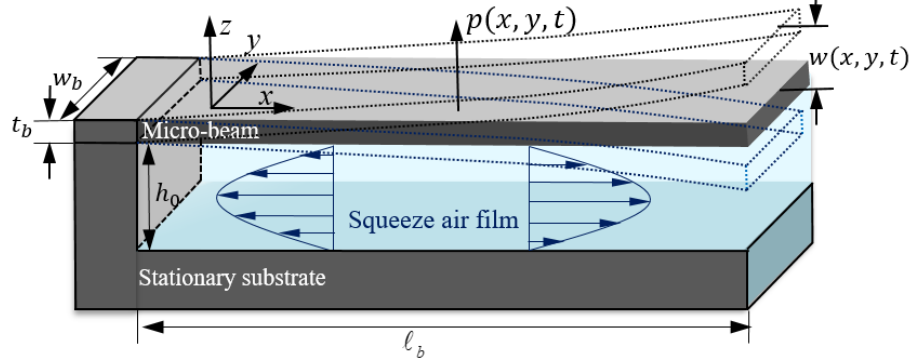


Figure 1. Dynamic vibration of MEMS beam resonators with their mode shapes under the SFD problem.

The pressure distribution of the SFD problem is obtained by solving the modified molecular gas film lubrication (MMGL) equation [14] as the following form

$$\frac{\partial}{\partial x} \left(\frac{\rho h^3}{12 \mu_{eff}(RH, T)} \frac{\partial p}{\partial x} \right) + \frac{\partial}{\partial y} \left(\frac{\rho h^3}{12 \mu_{eff}(RH, T)} \frac{\partial p}{\partial y} \right) = \frac{\partial}{\partial t} (\rho h) \quad (1)$$

where ρ is the density, h is the gas film spacing, p is the pressure, RH is the relative humidity of water vapor, and T is the temperature. Moist air, which involves water vapor and dry air, is applied in this study.

The effective viscosity (μ_{eff}) [19] of the gas flow is used to modify the MMGL equation considering the coupled effects of temperature and relative humidity in gas rarefaction as bellow

$$\mu_{eff} = \frac{\mu(RH, T, p)}{Q_p(D(RH, T, p), \alpha_1, \alpha_2)} \quad (2)$$

where μ is the dynamic viscosity of moist air, Q_p is the Poiseuille flow rate of gas flow in the gas rarefaction.

Moist air is a mixture of dry air and water vapor in which they are treated as an ideal gas mixture. In Dalton's model [20], the mixture pressure of moist air is calculated as follow

$$p = p_a + p_w \quad (3)$$

where p is total pressure of moist air (Pa), p_a is partial pressure of dry air (Pa), and p_w is partial pressure of water vapor (Pa).

To determine the amount of water vapor in moist air, the relative humidity (RH) [20, 21] is expressed as below

$$RH = \frac{P_w}{P_{sw}} \cdot 100\% \quad (4)$$

where p_{sw} is the saturation pressure of water vapor at the actual dry bulb temperature.

Specific humidity [20] is also used to describe the properties of moist air as below

$$x_s = 0.62198 \cdot p_w / (p - p_w) \quad (5)$$

where x_s is the specific humidity of moist air.

The saturation pressure of water vapor (p_{sw}) [22] is expressed as function of temperature as follow

$$p_{sw} = e^{(77.3450 + 0.0057T - 7235/T) / T^{8.2}} \quad (6)$$

The dynamic viscosity of moist air (μ) at low pressure [17] can be expressed as functions of pressure and temperature as follows

$$\mu = \frac{\mu_a}{1 + \Phi_{av} \cdot x_m} + \frac{\mu_v}{1 + \Phi_{va} / x_m} \quad (7)$$

where

$$\Phi_{av} = \frac{[1 + (\mu_a / \mu_v)^{0.5} \cdot (m_v / m_a)^{0.25}]^2}{2\sqrt{2} \cdot (1 + m_a / m_v)^{0.5}}, \quad \Phi_{va} = \frac{[1 + (\mu_v / \mu_a)^{0.5} \cdot (m_a / m_v)^{0.25}]^2}{2\sqrt{2} \cdot (1 + m_v / m_a)^{0.5}},$$

$x_m = 1.61 \times x_s$, $m_a (= 29)$ is molecular mass of dry air (kg/kmol), $m_v (= 18)$ is molecular mass of water vapor (kg/kmol).

The dynamic viscosity of dry air (μ_a) [17] under low pressure is

$$\mu_a = (a_1 + a_2 \cdot T - a_3 \cdot T^2 + a_4 \cdot T^3 - a_5 \cdot T^4) \times 10^{-6} \quad (8)$$

where $a_1 = 0.40401$, $a_2 = 0.074582$, $a_3 = 5.7171 \times 10^{-5}$, $a_4 = 2.9928 \times 10^{-8}$, $a_5 = 6.2524 \times 10^{-12}$.

The dynamic viscosity of water vapor (μ_v) [17] under low pressure is

$$\mu_v = (T / c_3)^{0.5} / (c_1 + c_2 \cdot (c_3 / T) + c_4 \cdot (c_3 / T)^2 - c_5 \cdot (c_3 / T)^3) \times 10^{-6} \quad (9)$$

where $c_1 = 0.0181583$, $c_2 = 0.0177624$, $c_3 = 647.27$, $c_4 = 0.0105287$, $c_5 = 0.0036744$.

The complete database of Poiseuille flow rate ($Q_p(D, \alpha_1, \alpha_2)$) [18] is used to modify the MMGL equation considering the gas rarefaction effects in wide range of inverse Knudsen number ($0.01 \leq D \leq 100$) and ACs ($0.1 \leq \alpha_1, \alpha_2 \leq 1.0$) conditions as follows:

$$\tilde{Q}_p(D, \alpha_1, \alpha_2) = \exp \left[\sum_{n=1}^{13} C_n (\ln D)^{13-n} \right] \quad (10)$$

$$Q_p = \frac{6}{D} \tilde{Q}_p \quad (11)$$

where $\tilde{Q}_p(D, \alpha_1, \alpha_2)$ is the Poiseuille flow rate for the gas rarefied flow.

The inverse Knudsen number (D), which is used as an important gas rarefaction indicator, is defined as follow

$$D = \frac{\sqrt{\pi}}{2K_n} = \frac{\sqrt{\pi}h}{2\lambda} \quad (12)$$

The mean free path of gas, which is estimated from kinetic theory of gases [21], can be estimated as follows

$$\lambda = \frac{RT}{\sqrt{2}\pi \cdot N_a d^2 p} = \frac{M}{\sqrt{2}\pi \cdot N_a d^2 \rho} \quad (13)$$

where $R = 8.314$ (J/mol) is the gas constant, $N_a = 6.0221 \times 10^{23}$ is the Avogadro's number, M is the molecular weight of gas and d is the diameter of the cross section of gas molecular at a stable state.

At ambient pressure condition, from Eqs. (3), (4) and (13), the mean free path of moist air (λ) can be expressed as functions of ambient pressure (p), temperature (T), and relative humidity (RH) as follows

$$\lambda = \frac{\lambda_0 p_0 T}{p T_0} = \frac{\lambda_0 p_0 T}{(p_a + RH \cdot p_{sw}) T_0} \quad (14)$$

where $\lambda_0 (= 65.5 \text{ nm})$ is reference mean free path of air at reference pressure of air ($p_0 = 101325$ Pa) and temperature ($T_0 = 300 \text{ K}$) condition.

2.2. Transverse vibration equation of MEMS beam resonators

In this section, we consider a transverse vibration of micro-beam resisted by a total pressure force ($p(x, y, t)$) of gas film per unit area of micro-beam in small gap spacing as shown in Figure 1. Under small displacement (w), we can obtain the following linear form of equation of motion that governs for the transverse displacement of the micro-beam [23] as follows

$$D_b \left(\frac{\partial^4 w}{\partial x^4} + 2 \frac{\partial^4 w}{\partial x^2 \partial y^2} + \frac{\partial^4 w}{\partial y^4} \right) + \rho_m t_b \frac{\partial^2 w}{\partial t^2} = -p(x, y, t) \quad (15)$$

where $D_b (= Et_b^3 / 12(1 - \nu^2))$ is the beam flexural rigidity, E is the Young's modulus, ν is the Poisson's ratio, t_b is the beam thickness, $w(x, y, t)$ is the transverse displacement at a positions along the beam (x, y), and time t , ρ_m is the material density of the beam. This equation is used to find the transverse displacement (w) of micro-beam.

The boundary conditions of the rectangular micro-beam are set with a clamped edge at one side ($x = 0$) as follows

$$w(0, y, t) = 0; \quad (16)$$

$$\frac{\partial w(0, y, t)}{\partial x} = 0 \quad (17)$$

and free edges at other sides ($x = \ell_b$ and $y = 0, y = w_b$) as follows

$$\frac{\partial^2 w(\ell_b, y, t)}{\partial x^2} = \frac{\partial^3 w(\ell_b, y, t)}{\partial x^3} = 0 \quad (18)$$

$$\frac{\partial^2 w(x, 0, t)}{\partial y^2} = \frac{\partial^3 w(x, 0, t)}{\partial y^3} = 0 \quad (19)$$

$$\frac{\partial^2 w(x, w_b, t)}{\partial y^2} = \frac{\partial^3 w(x, w_b, t)}{\partial y^3} = 0. \quad (20)$$

2.3. Quality factors of MEMS beam resonators

In this study, the quality factor of MEMS resonators is obtained by solving the MMGL equation in Eq. (1), the transverse vibration equation in Eq. (15) of micro-structure and their corresponding boundary conditions in Eqs.(16-20) simultaneously in the eigenvalue problem [12]. The Q -factor of MEMS resonators is calculated by obtaining the resultant eigenvalue ($\bar{\lambda} = \delta + i\omega$) by the Finite Element Method (FEM) [24]. The calculated procedures of the eigenvalue problem can be found in Section 2.5 of Nguyen and Li [12]. In the eigenvalue problems, the Q -factor of SFD (Q_{SFD}) can be evaluated as follows

$$Q_{SFD} = \frac{\omega_0}{2\delta} = \left| \frac{\text{Im}(\bar{\lambda})}{2\text{Re}(\bar{\lambda})} \right| \quad (21)$$

The total Q -factor (Q_T) can be evaluated by the main contributions of Q -factor of SFD (Q_{SFD}), TED (Q_{TED}), and support loss (Q_{sup}) [7, 12] as follows

$$\frac{1}{Q_T} = \frac{1}{Q_{SFD}} + \frac{1}{Q_{TED}} + \frac{1}{Q_{sup}} = \frac{1}{Q_{SFD}} + \frac{1}{Q_{int}} \quad (22)$$

where Q_{TED} is calculated by the Zener models [25, 26] as shown in Eq.(14) in [14] and the Lifshitz and Roukes (LR model) [27] in Eq.(15) in [14]. Q_{sup} is evaluated by the theoretical model of Hao et al. [28] as showed in Table 3 of Nguyen and Li [12].

Weighting of SFD ($Wt_{SFD}(\%)$), which is calculated as ratio of the contributions of the external SFD (Q_{SFD}^{-1}) and overall damping of SFD, TED (Q_{TED}^{-1}) and support loss (Q_{sup}^{-1}) as follow

$$Wt_{SFD}(\%) = \frac{(Q_{SFD})^{-1}}{(Q_T)^{-1}} = \frac{(Q_{SFD})^{-1}}{(Q_{SFD})^{-1} + (Q_{int})^{-1}} \quad (23)$$

where $(Q_{int})^{-1} = (Q_{TED})^{-1} + (Q_{sup})^{-1}$ is the internal structural damping of MEMS resonators.

3. RESULTS AND DISCUSSION

3.1. Effective viscosity, $\mu_{eff}(RH, T)$

In Figure 2, the saturated pressure of water vapor (p_{sw}) is plotted as function of temperature (T). The results shown that p_{sw} increases as T increases in wide range of temperature ($200 \text{ K} \leq T \leq 380 \text{ K}$). The results can be applied to calculate the variations of relative humidity of moist air (in Eq. (4)) in wide range of ambient pressure and temperature conditions.

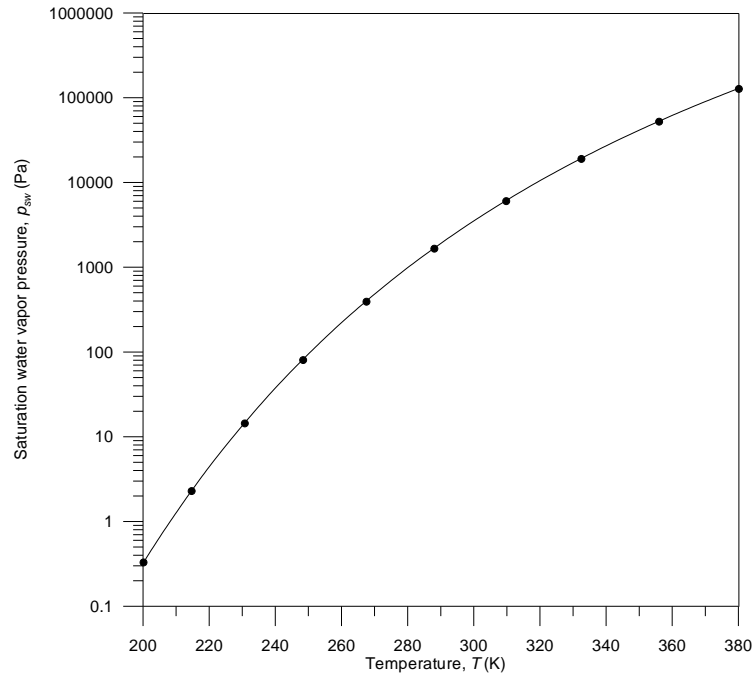


Figure 2. Saturation pressure of water vapor (p_{sw}) versus ambient temperature (T).

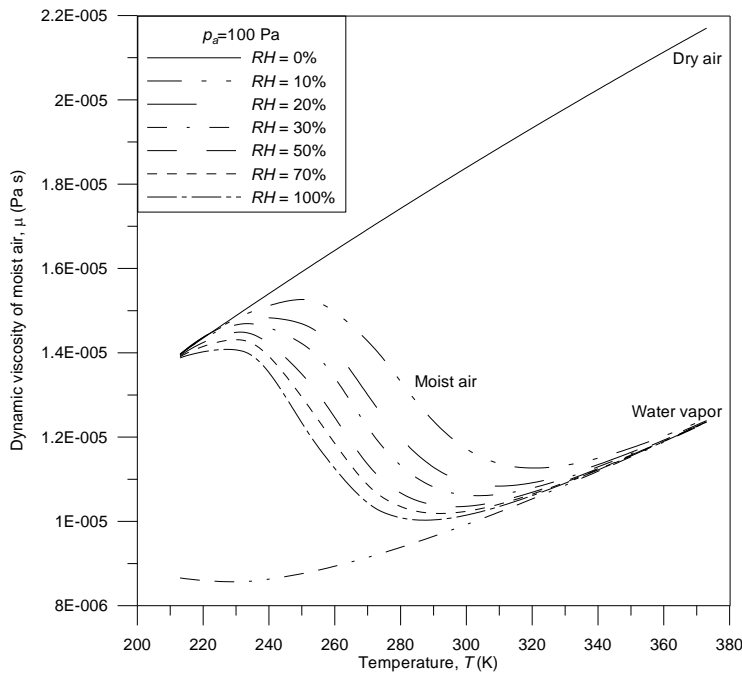


Figure 3. Dynamic viscosity of moist air (μ) versus ambient temperature (T) for different relative humidity (RH) at high gas rarefaction ($p_a = 100 \text{ Pa}$).

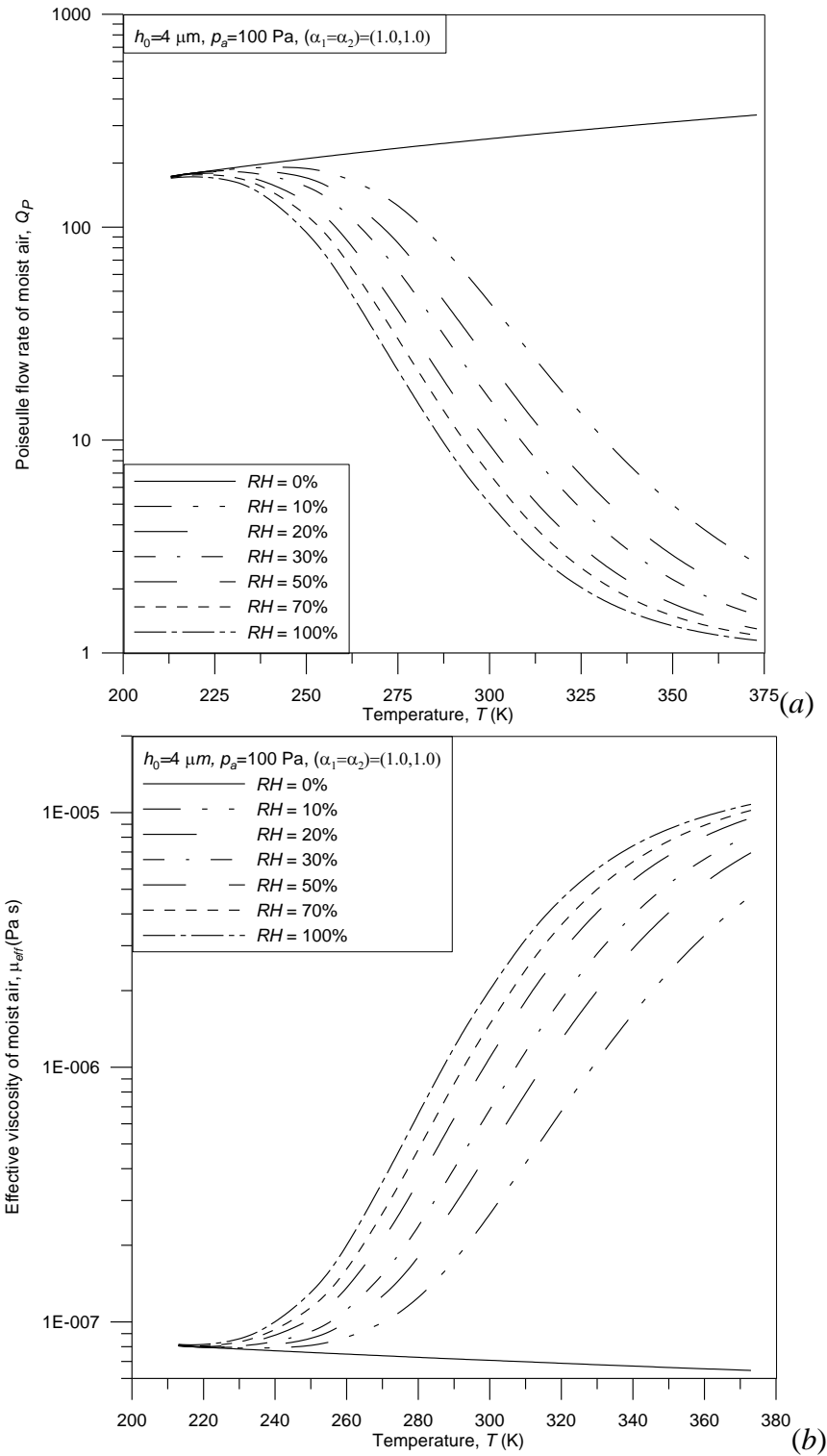


Figure 4. (a) Poiseuille flow rate (Q_p), (b) effective viscosity (μ_{eff}) of moist air versus ambient temperature (T) for different relative humidity (RH) at high gas rarefaction ($p_a = 100$ Pa).

In Figure 3(a), the dynamic viscosity of moist air (μ) in Eq. (7), dry air (μ_a) in Eq. (8), and water vapor (μ_v) in Eq. (9) are plotted as functions of temperature (T) and relative humidity (RH) at high gas rarefaction ($p_a = 100$ Pa), respectively. The results shown that both of μ_a and μ_v increase with T . Thus, μ increases slightly with T because μ_a increases with T . Also, μ decreases significantly, and then increases to approach μ_v as T increases because μ_v increases with T . Furthermore, μ decreases as relative humidity (RH) increases in wide range of temperature (T) conditions.

In Figure 4(a), the Poiseuille flow rate (Q_p) of moist air (Eq.(11)) and effective viscosity (μ_{eff}) (Eq.(2)) are plotted as functions of temperature (T) for different relative humidity (RH) at high gas rarefaction ($p_a = 100$ Pa). The results shown that Q_p of dry air increases slightly with T , while Q_p of moist air decreases significantly as T increases. Also, Q_p of moist air decreases as RH increases. Furthermore, influence of RH on Q_p becomes more significantly at higher T conditions. In figure 4 (b), The results shown that μ_{eff} decreases slightly as T increases, while μ_{eff} increases significantly with T because Q_p decreases significantly with T . Also, μ_{eff} increases as RH increases because Q_p decreases as RH increases in wide range of T . Thus, the obtained results can be used to discuss the coupled effects of temperature and relative humidity on the quality factors of MEMS resonators in gas rarefaction (p , and ACs(α_1, α_2)) conditions.

3.2. Influences of temperature and relative humidity of moist air on Q_{SFD}

In this result, the dimensions of beam are used by the length $\ell_b = 350$ μm , the width $w_b = 22$ μm , and the thickness $t_b = 4$ μm which are used as same as dimension of the micro-beam shown in Nguyen and Li [12]. The material properties of polysilicon [29, 30] are the Young's modulus $E = 160 \times 10^9$ Pa, density $\rho_m = 2330$ Kg/m^3 , Poisson's ratio $\nu = 0.22$, thermal expansion coefficient $\alpha_m = 2.6 \times 10^{-6}$ 1/K, thermal conductivity $\kappa = 90$ W/(m.K), specific heat capacity $C_p = 700$ J/(kg. K). Basic operating conditions of gas film are used with thickness of gas film $h_0 = 4$ μm , pressure $p_a = 100$ Pa. In Figure 5, the damping factor (δ_{SFD}) and the Q -factor of SFD (Q_{SFD}) ($= \omega_n / 2\delta_n$) in Eq. (21), are plotted as functions of temperature (T) and relative humidity (RH) at the 1st mode of vibration and high gas rarefaction ($p_a = 100$ Pa) condition. In figure 5 (a), the results shown that the damping factor (δ_{SFD}) of dry air decreases slightly as T increases, whereas δ_{SFD} of moist air increases more significantly as T and RH increase because Q_p of dry air increases slightly as T increases, while Q_p of moist air decreases significantly as T and RH increase. In Figure 5 (b), the resultant Q -factor of SFD (Q_{SFD}) of dry air increases slightly with T . While, Q_{SFD} of moist air decreases significantly as T and RH increase at high gas rarefaction ($p_a = 100$ Pa) condition. Thus, the influences of temperature and relative humidity on the Q -factors of MEMS resonators must be carefully considered in wide range of resonant mode of vibration and gas rarefaction (p_a and ACs ($\alpha_1 = \alpha_2$)) conditions.

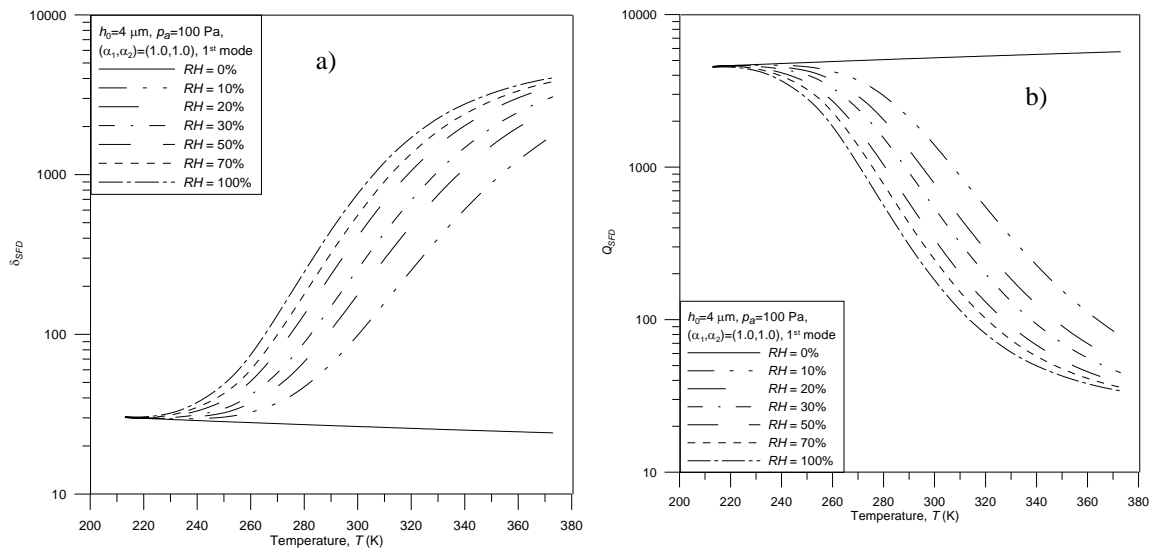


Figure 5. (a) damping factor of SFD (δ_{SFD}) and (b) Q -factor of SFD (Q_{SFD}) versus ambient temperature (T) for different relative humidity (RH) in high gas rarefaction ($p_a=100 \text{ Pa}$).

3.3. Influences of temperature and relative humidity of moist air on Q_T and $Wt_{SFD}(\%)$

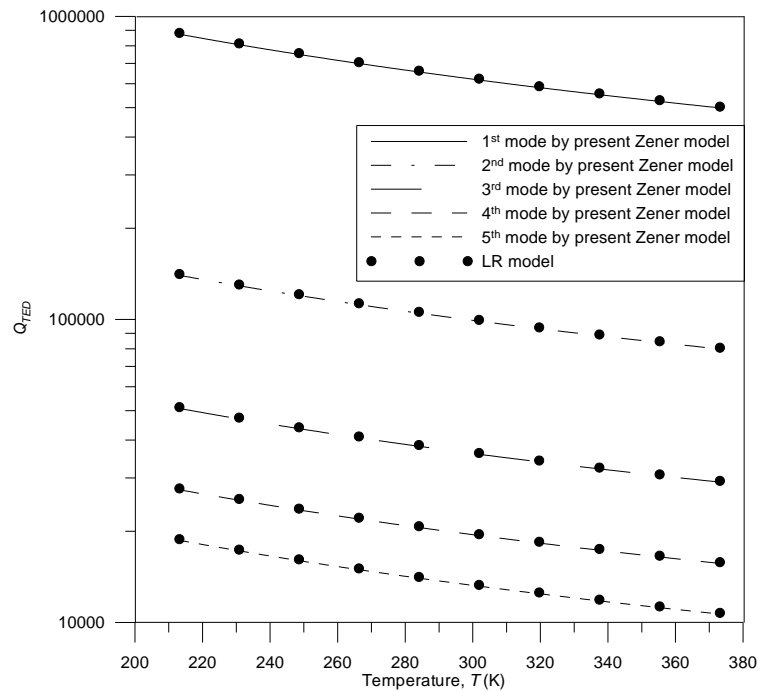


Figure 6. The Q -factor of TED (Q_{TED}) versus temperature (T) for different mode of resonator and comparisons with Zener model [25, 26] and LR model [27].

In Figure 6, the Q factor of TED (Q_{TED}) is calculated as function of temperature (T) for various resonant modes of vibration. The result showed that Q_{TED} decreases as T increases for different resonant modes of vibration. Also, Q_{TED} decreases more significantly as the resonant

mode of vibration increases because the TED increases and becomes dominantly in higher resonant frequencies conditions. The calculated results of Q_{TED} from the LR model [27] showed good agreement with those obtained results from the Zener model [25, 26] in wide range of T and resonant mode of vibration condition.

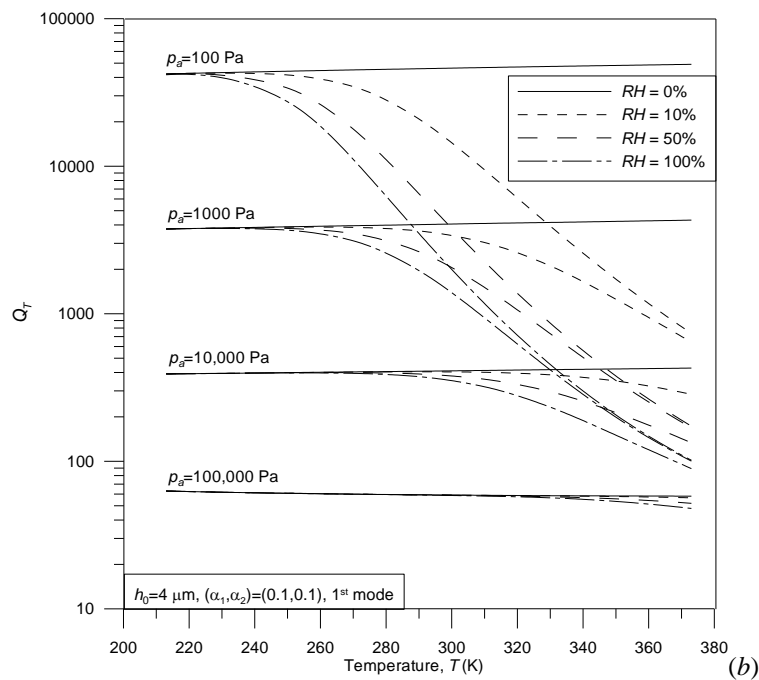
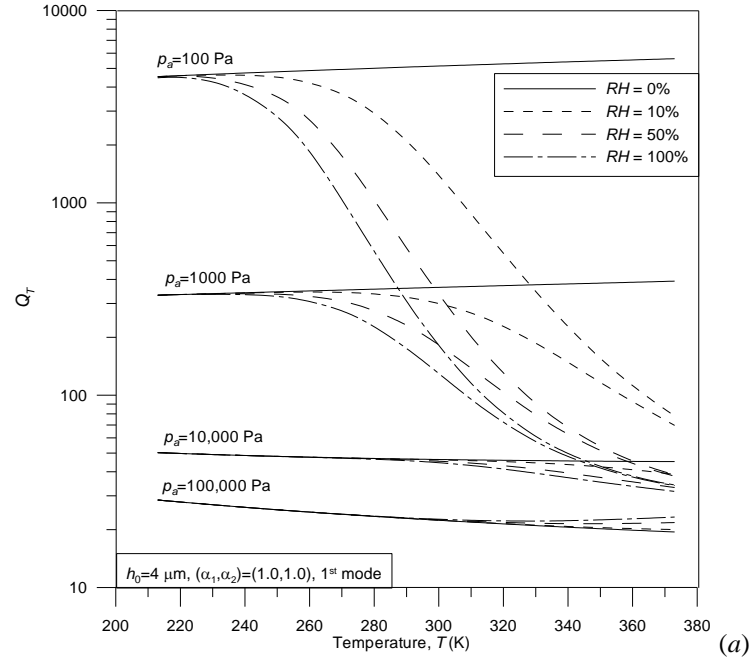


Figure 7. Total Q -factor (Q_T) versus temperature (T) and relative humidity (RH) for different pressure (p_a) for (a) ACs(1.0,1.0), and (b) ACs(0.1,0.1).

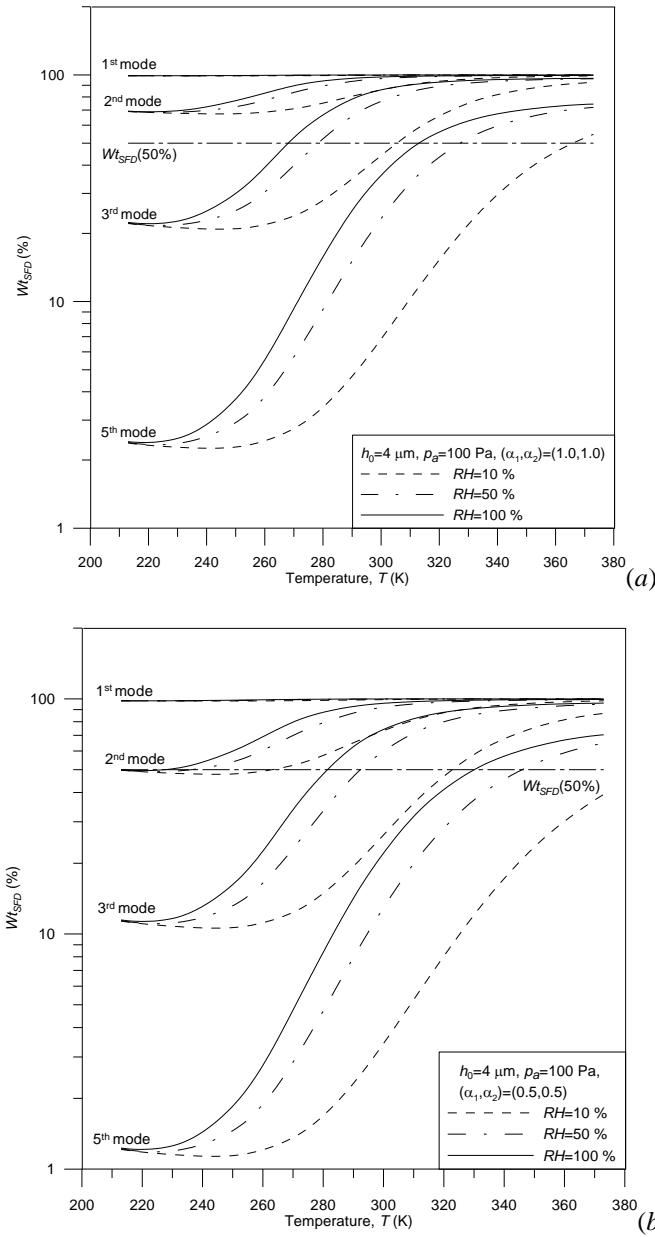


Figure 8. Weighting of SFD ($Wt_{SFD}(\%)$) versus temperature (T) and relative humidity (RH) with different mode of vibration for gas rarefaction, (a) ACs(1.0,1.0), and (b) ACs(0.5,0.5).

In Figure 7, the total Q -factor (Q_T), which is calculated by Eq.(22) by the contributions of Q -factor of SFD, TED (figure 6) and support loss (Table 3 in Nguyen and Li [12]), respectively, is plotted as functions of temperature (T) and relative humidity (RH) for different gas rarefaction (p_a , and ACs (α_1, α_2)) conditions. In the 1st mode of vibration, the SFD is dominant damping source in calculations of Q_T of MEMS resonators [12, 31]. In Figure 7(a), Q_T of moist air decreases more significantly as T and RH increase because Q_p decreases more significantly than that of μ as T and RH increase at high gas rarefaction ($p_a = 100 \text{ Pa}$, 1000 Pa , $10,000 \text{ Pa}$). Also, the influence of RH on Q_T are reduced and can be neglected at lower gas rarefaction (higher p_a)

because μ changes with RH and T more dominantly than that of Q_p in lower gas rarefaction (higher p_a). Whereas, this influence of RH on Q_T becomes more significantly at lower p_a and higher T because Q_p of moist air changed with RH and T more dominantly than that of μ in lower p_a and higher T conditions. Furthermore, the coupled effects of T and RH on Q_T become more dominantly as the ACs decrease from ACs(1.0,1.0) (Figure 7(a)) to ACs(0.1,0.1) in Figure 7(b). The influence of RH on Q_T becomes significantly in higher gas rarefaction (lower p_a , and ACs(α_1, α_2)) and higher T , while this influence decreases and can be neglected in lower gas rarefaction (higher p_a , and ACs(α_1, α_2)) and lower temperature (T) conditions. Thus, it's possible to design for the higher Q -factor of MEMS resonators under the influence of relative humidity of moist air environment in lower temperature and higher gas rarefaction (lower p_a and ACs ($\alpha_1 = \alpha_2$)) conditions.

In Figure 8, Weighting of SFD ($W_{t_{SFD}}(\%)$) of moist air in Eq. (23) is introduced to investigate the coupled effects of temperature (T) and relative humidity (RH) on the dynamic performance of MEMS resonators in wide range of resonant mode of vibration and higher gas rarefaction ($p_a = 100$ Pa) conditions. In Figure 8(a), $W_{t_{SFD}}(\%)$ increases as T and RH increase because the SFD increases and the gas flow becomes more restricted as T and RH increase. Furthermore, influence of relative humidity on $W_{t_{SFD}}(\%)$ seems unchanged in the 1st mode of vibration in which the SFD is very dominant on total damping (Q_T)⁻¹.

Whereas, influences of RH on $W_{t_{SFD}}(\%)$ becomes more significantly as the mode of vibration increases because the contribution of SFD, (Q_{SFD})⁻¹ reduces significantly, while the contribution of TED, (Q_{TED})⁻¹ and support loss, (Q_{sup})⁻¹ on (Q_T)⁻¹ becomes more dominantly at higher mode of resonators. Furthermore, the influences of T and RH on $W_{t_{SFD}}(\%)$ become more considerably in wide range of mode of vibration as the gas rarefaction increases from ACs(1.0,1.0) in Figure 8(a) to ACs(0.5,0.5) in Figure 8(b). Thus, the coupled effects of temperature (T) and relative humidity (RH) on $W_{t_{SFD}}(\%)$ become more significantly at higher resonator modes and higher gas rarefaction (lower p_a and ACs (α_1, α_2)) conditions. The obtained results of $W_{t_{SFD}}(\%)$ can be used to design the higher Q -factor and high sensitivity of chemical sensors to detect the humidity of moist air in higher resonant modes, higher gas rarefaction (lower p_a and ACs ($\alpha_1 = \alpha_2$)) and in wide range of temperature conditions.

4. CONCLUSIONS

In this study, the coupled effects of temperature (T) and relative humidity (RH) on Q_{SFD} , Q_T , and $W_{t_{SFD}}(\%)$ of MEMS resonators are discussed in wide range of relative humidity ($0\% \leq RH \leq 100\%$), temperature ($200 \leq T \leq 380$), inverse Knudsen number ($0.01 \leq D \leq 100$), and ACs ($0.1 \leq \alpha_1, \alpha_2 \leq 1.0$) conditions. Some remarkable outcomes were listed as below:

- a. Q_{SFD} of moist air decreases more significantly as temperature (T) and relative humidity (RH) increase at higher gas rarefaction (lower p_a) in the 1st mode of vibration.
- b. Influence of relative humidity (RH) on Q_{SFD} , Q_T , and $W_{t_{SFD}}(\%)$ becomes more significantly in higher gas rarefaction (lower p_a , and ACs(α_1, α_2)) and higher temperature (T), while this influence decreases and can be neglected in lower gas rarefaction (higher p_a , and ACs(α_1, α_2)) and lower temperature (T) conditions in the 1st mode of vibration.

- c. The coupled effects of temperature (T) and relative humidity (RH) on $Wt_{SFD}(\%)$ are neglected at the 1st mode of resonator, while this influence becomes more significantly at higher resonator modes and higher gas rarefaction (lower p_a and ACs (α_1, α_2)) conditions.

Acknowledgements. This research was supported by the annual projects of The Research Laboratories of Saigon High Tech Park in 2019 according to decision No. 102/QĐ-KCNC of Management Board of Saigon High Tech Park and contract No. 01/2019/HĐNVTX-KCNC-TTRD (Project number 3).

REFERENCES

1. Baller M. K., Lang H. P., Fritz J., Gerber Ch., Gimzewski J. K., Drechsler U., Rothuizen H., Despont M., Vettiger P., Battiston F. M., Ramseyer J. P., Fornaro P., Meyer E., and Güntherodt H. J. – A cantilever array-based artificial nose, *Ultramicroscopy* **82** (1-4) (2000) 1-9.
2. Lang H. P., Hegner M., and Gerber C. – Cantilever array sensors, *materialstoday* **8** (4) (2005) 30-36.
3. Hosaka H., Itao K., and Kuroda S. – Damping characteristics of beam-shaped micro-oscillators, *Sensor. Actuat. A-Phys.* **49** (1-2) (1995) 87–95.
4. Zhou H., Li P., and Zuo W. – Thermoelastic damping in micro-wedged cantilever resonator with rectangular cross-section, *Proceedings of the 2016 IEEE International Conference on Mechatronics and Automation*, (2016) 1590-1595.
5. Jandak M., Neuzil T., Schneider M., and Schmid U. – Investigation on different damping mechanisms on the Q factor of MEMS resonators, *Procedia Engineering* **168** (2016) 929-932.
6. Nieva P. M., McGruer N. E., and Adams G. G. – Design and characterization of a micromachined Fabry–Perot vibration sensor for high-temperature applications, *J. Micromech. Microeng.* **16** (2006) 2618–2631.
7. Kim B., Hopcroft M. A., Candler R. N., Jha C. M., Agarwal M., Melamud R., Chandorkar S. A., Yama G., and Kenny T. W. – Temperature dependence of quality factor in MEMS resonators, *J. Microelectromech. S.* **17** (3) (2008) 755–766.
8. Ghaffari S., Ng E. J., Ahn C. H., Yang Y., Wang S., Hong V. A., and Kenny T. W. – Accurate modeling of quality factor behavior of complex silicon MEMS resonators, *J. Microelectromech. S.* **24** (2) (2015) 276–288.
9. Hosseinzadegan H., Pierron O. N., and Hosseinian E. – Accurate modeling of air shear damping of a silicon lateral rotary micro-resonator for MEMS environmental monitoring applications, *Sensor. Actuat. A-Phys.* **216** (2014) 342–348.
10. Jan M. T., Ahmad F., Hamid N. H. B., Khir M. H. B. M., Shoaib M., and Ashraf K. – Experimental investigation of temperature and relative humidity effects on resonance frequency and quality factor of CMOS-MEMS paddle resonator, *Microelectron. Reliab.* **63** (2016) 82–89.
11. Hasan M. H., Ouakad H. M., and Alsaleem F. – On the effects of temperature and relative humidity on the response of a MEMS arch resonator, *Proceedings of ASME 2017 International Design Engineering Technical Conferences and Computers and Information in Engineering Conference*, (2017) 1-10.

12. Nguyen C. C., and Li W. L. – Effect of gas rarefaction on the quality factors of micro-beam resonators, *Microsyst. Technol.* **23** (8) (2017) 3185–3199.
13. Nguyen C. C., and Li W. L. – Effects of surface roughness and gas rarefaction on the quality factor of micro-beam resonators, *Microsyst. Technol.* **23** (8) (2017) 3489–3504.
14. Nguyen C. C., and Li W. L. – Influences of temperature on the quality factors of micro-beam resonators in gas rarefaction, *Sensor. Actuat. A-Phys.* **261** (2017) 151–165.
15. Haider S. T., Saleem M. M., and Ahmad M. – FEM Modeling of Squeeze Film Damping Effect in RF-MEMS Switches, *Proceedings of EECSI 2017, Yogyakarta, Indonesia, (2017).*
16. Nguyen C. C., Ngo V. K. T., Le H. Q., and Li W. L. – Influences of relative humidity on the quality factors of MEMS cantilever resonators in gas rarefaction, *Microsyst. Technol.* **23** (8) (2018) 1–16.
17. Morvay Z. K., and Gvozdenac D. D. – *Applied Industrial Energy and Environmental Management, Fundamentals for analysis and calculation of energy and environmental performance*, John Wiley & Sons, Ltd, 2008, 1-5.
18. Li W. L. – A database for interpolation of Poiseuille flow rate for arbitrary Knudsen number lubrication problems, *J. Chin. Inst. Eng.* **26** (4) (2003) 455–466.
19. Veijola T., Kuisma H., Lahdenperä J., and Ryhänen T. – Equivalent-circuit model of the squeezed gas film in a silicon accelerometer, *Sensor. Actuat. A-Phys.* **48** (3) (1995) 239–248.
20. Kreith F., and Goswami D. Y. – *The CRC HANDBOOK of Mechanical engineering*, CRC Press LLC, 2005, 1385.
21. Tan Z. – *Air Pollution and Greenhouse Gases*, Springer Science+Business Media, Singapore, 2014, 39-40.
22. ASHRAE – *The 2001 ASHRAE Fundamentals Handbook*, 2001, 6.2 (Eq.5).
23. Leissa A. W., *Vibration of Plates*, NASA, Washington, DC, 1969 (Eq.1.1).
24. Reddy J. N., *An introduction to the finite element method*, McGraw-Hill, New York, 1993.
25. Zener C. – Internal friction in solids. I. Theory of internal friction in reeds, *Phys. Rev.* **52** (3) (1937) 230–235.
26. Zener C. – Internal friction in solids II. General theory of thermoelastic internal friction, *Phys. Rev.* **53** (1) (1938) 90–99.
27. Lifshitz R., and Roukes M. L. – Thermoelastic damping in micro- and nanomechanical systems, *Phys. Rev. B* **61** (8) (2000) 5600-5609.
28. Hao Z., Erbil A., and Ayazi F. – An analytical model for support loss in micromachined beam resonators with in-plane flexural vibrations, *Sensor. Actuat. A-Phys.* **109** (1–2) (2003) 156–164.
29. Pandey A. K., and Pratap R. – Effect of flexural modes on squeeze film damping in MEMS cantilever resonators, *J. Micromech. Microeng.* **17** (2007) 2475-2484.
30. Matthew A. H., William D. N., and Thomas W. K. – What is the Young’s Modulus of Silicon?, *J. Microelectromech. S.* **19** (2) (2010) 229-238.
31. Li W. L., – Analytical modelling of ultra-thin gas squeeze film, *Nanotechnology* **10** (1999) 440–446.